



Impacts of meteorology and emissions on surface ozone increases over Central Eastern China between 2003 and 2015

Lei Sun^{1,2}, Likun Xue^{1*}, Yuhang Wang^{2*}, Longlei Li², Jintai Lin³, Ruijing Ni³, Yingying Yan^{3,4},
Lulu Chen³, Juan Li¹, Qingzhu Zhang¹, Wenxing Wang¹

5 ¹Environment Research Institute, Shandong University, Ji'nan, Shandong, China

²School of Earth and Atmospheric Sciences, Georgia Institute of Technology, Atlanta, GA, USA

³Laboratory for Climate and Ocean-Atmosphere Studies, Department of Atmospheric and
Oceanic Sciences, School of Physics, Peking University, Beijing, China

⁴Department of Atmospheric Sciences, School of Environmental Studies, China University of
10 Geosciences (Wuhan), 430074, Wuhan, China

Correspondence to:

Likun Xue (xuelikun@sdu.edu.cn) and Yuhang Wang (yuhang.wang@eas.gatech.edu)

Abstract

Recent studies have shown that surface ozone (O₃) concentrations over Central Eastern China
15 (CEC) have increased significantly during the past decade. We quantified the effects of changes
in meteorological conditions and O₃ precursor emissions on surface O₃ levels over CEC between
July 2003 and July 2015 using the GEOS-Chem model. The simulated monthly mean maximum
daily 8-h average O₃ concentration (MDA8 O₃) in July increased by approximately 13.6%, from
65.5±7.9 ppbv (2003) to 74.4±8.7 ppbv (2015), comparable to the observed results. The change
20 in meteorology led to an increase of MDA8 O₃ of 5.8±3.9 ppbv over the central part of CEC, in
contrast to a decrease of about -0.8±3.5 ppbv over the eastern part of the region. In comparison,
the MDA8 O₃ over the central and eastern parts of CEC increased by 3.5±1.4 ppbv and 5.6±1.8
ppbv due to the increased emissions. The increase in regional averaged O₃ resulting from the
emission increase (4.0±1.9 ppbv) was higher than that caused by meteorological changes
25 (3.1±4.9 ppbv) relative to the 2003 standard simulation, while the regions with larger O₃
increases showed a higher sensitivity to meteorological conditions than to emission changes.
Sensitivity tests indicate that increased levels of anthropogenic non-methane volatile organic
compounds (NMVOCs) dominate the O₃ increase over the eastern part of CEC, and
anthropogenic nitrogen oxides (NO_x) mainly increase O₃ concentrations over the central and



western parts, while decrease O₃ in a few urban areas in the eastern part. Process analysis showed that net photochemical production and meteorological conditions (transport in particular) are two important factors that influence O₃ levels over the CEC. The results of this study suggest a need to further assess the effectiveness of control strategies for O₃ pollution in the context of regional meteorology, transboundary transport, and anthropogenic emission changes.

1. Introduction

Tropospheric ozone (O₃) is a major atmospheric oxidant and the primary source of hydroxyl radicals (OH), which control the atmospheric oxidizing capacity (Seinfeld and Pandis, 2016). In the troposphere, O₃ is produced by the photochemical oxidation of hydrocarbons, carbon monoxide (CO) and nitrogen oxides (NO_x) in the presence of sunlight, and can be transported from the stratosphere (Crutzen, 1973; Danielsen, 1968). It is an important greenhouse gas with a positive radiative forcing of 0.4 (0.2–0.6) W m⁻² (IPCC, 2013), and it has adverse effects on human health and ecosystem productivity (Monks et al., 2015).

Surface O₃ concentrations increased globally during the 20th century. Almost all available monitoring data from 1950–1979 until 2000–2010 for the Northern Hemisphere indicate an increase of 1–5 ppbv per decade (Cooper et al., 2014; Monks et al., 2015), although the trends have varied regionally since the 1990s. The O₃ concentrations in rural and remote areas of Europe showed an increasing trend until 2000, but then tended to level off or decline (Oltmans et al., 2013; Parrish et al., 2014; Yan et al., 2018b). In the eastern US, summertime O₃ has continued declining since 1990, whereas springtime O₃ in the western US shows large inter-annual variability (Lin et al., 2015). At some remote sites of western US, only small increases (0.00–0.43 ppbv yr⁻¹) have been recorded (Cooper et al., 2012). In comparison with Europe and North America, the O₃ concentrations in China have shown significant increasing trends since the 1990s. Ding et al. (2008) reported an increase of 3 ppbv yr⁻¹ in the afternoon boundary-layer O₃ concentrations in summer over Beijing using aircraft data obtained by the Measurement of Ozone and Water Vapor by Airbus In-Service Aircraft (MOZAIC) program during 1995–2005. The maximum daily 8-h average O₃ concentration (MDA8 O₃) at Shangdianzi, a rural site near Beijing, showed a significant increase at a rate of about 1.1 ppbv yr⁻¹ from 2003 to 2015 (Ma et al., 2016). Sun et al. (2016) reported an increase of 1.7–2.1 ppbv yr⁻¹ at Mt Tai during summertime from 2003 to 2015. In recent years, high O₃ concentrations



have been widely observed in China, especially in the Central Eastern China (CEC: 103 °E to 120 °E, 28 °N to 40 °N) during the summertime (Wang et al., 2006; 2017; Xue et al., 2014). All of these results indicate that CEC might continue to experience worsening O₃ air pollution. In this study, we quantify the effects of several factors on O₃ changes and propose some suggestions to control surface O₃ in the future.

The level of O₃ in the troposphere is mainly determined by the abundance of its precursors, including both anthropogenic and natural emissions, and the meteorological conditions (Logan, 1985). The anthropogenic NO_x emissions in China continued rising until the launch of the Twelfth Five-Year Plan (2011–2015), which enforced a series of stringent NO_x emission control measures (China State Council, 2011). However, anthropogenic emissions of non-methane volatile organic compounds (NMVOCs) continue to increase unabated (Li et al., 2017a; Zheng et al., 2018). Biomass burning also makes an important contribution to O₃ formation (Real et al., 2007; Yamaji et al., 2010), and biogenic emissions of isoprene and monoterpenes contribute to O₃ levels, which are influenced by meteorological variations (Fu and Liao, 2012). Meteorological parameters, such as wind, temperature and humidity, can influence O₃ concentrations via mechanisms related to transport, chemical production and loss, and deposition (Monks, 2000; Zhao et al., 2010). Studies in the past two decades have shown that O₃ and its precursors can be transported across regions and even hemispheres, as it has a lifetime of several days to weeks in the troposphere (Jacob et al., 1999; Lin et al., 2008; Verstraeten et al., 2015). For example, Ni et al. (2018) showed significant foreign contributions to springtime O₃ over China. In addition, the stratosphere–troposphere exchange (STE) is another important process affecting the tropospheric O₃ burden, especially in the mid-latitudes of the Northern Hemisphere during springtime (Hess and Zbinden, 2013). However, currently there is still large variation in quantifying the contribution of each factor to the O₃ trends among different models and study regions (Zhang et al., 2014a).

Previous studies have revealed the important effects of changing emission levels and varying climate conditions on tropospheric O₃ in different regions. Lou et al. (2015) found that the effect of variations in meteorological conditions on the inter-annual variability of surface O₃ was larger than that of variations in anthropogenic emissions in Eastern China from 2004–2012. Using the GEOS-Chem model, Yan et al. (2018a) found that inter-annual climate variability is the main driver of daytime O₃ variability in the US, although the reduction of anthropogenic emissions of



NO_x increased the night-time O₃ concentrations due to reduced O₃ titration. The effects of East Asian summer monsoon on surface O₃ have been analyzed by observational and modeling studies (He et al., 2008; Wang et al., 2011; Zhao et al., 2010). Given the scarcity of previous research, it is necessary to further quantify the contributions of emissions and meteorological
5 conditions to surface O₃ levels to deepen our understanding of the factors influencing O₃ changes in China.

This study integrates the global GEOS-Chem model and its Asia nested model to investigate the spatial distributions of surface O₃ over CEC in July 2003 and July 2015. Meteorological conditions and O₃ precursor emissions are identified as the dominant factors influencing O₃
10 levels, and their contributions are quantified. We identify the key factors that affect O₃ changes and make a policy recommendation for O₃ control over CEC in the future. Section 2 briefly introduces the GEOS-Chem model and simulation scenarios. Comparisons of the simulated and observed O₃ concentrations are made in Section 3. We quantify the individual effects of meteorological conditions and emissions on O₃ changes in Section 4 and Section 5, respectively.
15 In Section 6, we discuss important processes influencing O₃ changes. Section 7 concludes the paper.

2. Model and simulations

2.1 Model description

A nested model coupled with the global chemical transport model GEOS-Chem v11-01
20 (<http://acmg.seas.harvard.edu/geos/doc/man/>), is used to simulate the surface O₃ concentrations and distributions over CEC in July of 2003 and 2015. The meteorological field is taken from MERRA-2 as assimilated by the Goddard Earth Observing System (GEOS) at NASA's Global Modelling and Assimilation Office. The global model and its nested model, covering China and South East Asia (60 °E to 150 °E, 11 °S to 55 °N), are configured to have horizontal spatial
25 resolutions of 2 ° × 2.5 ° and 0.5 ° × 0.625 °, respectively, by latitude and longitude, and 47-layer reduced grids in the vertical direction with 10 layers (each ~130 m in thickness) below 850 hPa. The models are run with the full standard NO_x-O_x-hydrocarbon-aerosol tropospheric chemistry (Mao et al., 2013) for January to July of 2003 and 2015, including the spin-up time, but only the results for July are analysed. We use the Linoz stratospheric ozone chemistry mechanism for
30 stratospheric O₃ production (McLinden et al., 2000), and the non-local planetary boundary layer



(PBL) mixing scheme for vertical mixing of air tracers in the PBL (Holtstlag and Boville, 1993; Lin and McElroy, 2010).

Global anthropogenic emissions of NO_x and CO for 2003 and 2008 are taken from EDGAR v4.2 (Emission Database for Global Atmospheric Research, <http://edgar.jrc.ec.europa.eu/overview.php?v=42>). NMVOC emissions are taken from the RETRO (REanalysis of TROpospheric chemical composition) inventory for 2000, but the emissions of C₂H₆ and C₃H₈ follow Xiao et al. (2008). For Europe, the United States, Asia, China, Canada and Mexico, the anthropogenic emissions are taken from EMEP (from 2003 to 2012; Auvray et al., 2005), NEI2011 (base year: 2011, annual scale factors: 2006–2013; <ftp://aftp.fsl.noaa.gov/divisions/taq/>), MIX (from 2008 to 2010; Li et al., 2017b), MEIC (2008 and 2014, <http://meicmodel.org>), CAC (NO_x and CO: from 2003 to 2008 (scaled to 2010); http://www.ec.gc.ca/pdb/cac/cac_home_e.cfm), and BRAVO (1999; Kuhns et al., 2003), respectively. Over China, the CO, NO_x and NMVOC emissions from MEIC for 2008 are scaled to 2003 based on the inter-annual variability of Regional Emission in Asia (REAS-v2; Kurokawa et al., 2013), but the anthropogenic emissions for 2014 are taken directly without being scaled to 2015. According to Zheng et al. (2018), the anthropogenic NO_x and NMVOC emissions in China decreased by about 6% and 2% from 2014 to 2015, respectively, so here we may slightly overestimate the NO_x and NMVOC emissions. Daily biomass burning emissions are taken from the Global Fire Emission Database v4 (GFED4) (Randerson et al., 2012). Biogenic emissions in the GEOS-Chem model are calculated online from the MEGAN v2.1 scheme (Guenther et al., 2012). Natural NO_x emissions from lightning are parameterised following Price and Rind (1992), and are further constrained by the LIS/OTD satellite data (Murray et al., 2012). We obtain the vertical profile of the lightning NO_x based on Ott et al. (2010) and calculate the soil NO_x emissions online following Hudman et al. (2012).

2.2 Model simulations

Table 1 summarises the six model scenarios we set to identify the contributions from the changes in meteorological conditions and emissions between 2003 and 2015. We refer to the scenario using the emissions described in the previous section as the standard simulation, and define the standard simulations for 2003 and 2015 as 03E03M and 15E15M (2003 emissions + 2003 meteorology and 2015 emissions + 2015 meteorology). In this case, the difference between



O₃ concentrations for 03E03M and 15E15M (denoted as 15E15M-03E03M) is due to the combined effect of changes in emissions and meteorology between 2003 and 2015. Similarly, scenarios with 2003 emissions + 2015 meteorology and 2015 emissions + 2003 meteorology are defined as 03E15M and 15E03M, respectively. The contribution of the change in meteorological
5 conditions can thus be calculated by the difference between the simulated O₃ concentrations in the 03E15M and 03E03M scenarios (03E15M-03E03M). Similarly, the contribution of emission changes can be calculated by 15E03M-03E03M (or 15E15M-03E15M). The contribution of the meteorological change based on the 2015 standard simulation is given by 15E15M-15E03M. Since the amount of O₃ formed responds nonlinearly to the NO_x and NMVOC emissions, the
10 sum of (03E15M-03E03M) and (15E03M-03E03M) does not equal to (15E15M-03E03M). However, we can still compare these two scenarios to quantify the effects of meteorology and emission changes.

We then investigate the effect of anthropogenic emissions (NO_x and NMVOCs) on surface O₃ concentrations based on the 2015 simulations. We replace the anthropogenic NO_x or NMVOC
15 emissions in the 2015 standard simulation with corresponding emissions for 2003 and keep the meteorology field, biomass burning, and natural emissions (NO_x from soil and lightning, biogenic VOCs (BVOCs), etc.) unchanged (03N15M and 03V15M, respectively). The contribution of anthropogenic NO_x (NMVOCs) emission changes can be calculated by the difference between the 2015 standard simulation and 03N15M (03V15M), defined as
20 15E15M-03N15M (15E15M-03V15M).

3. Simulated and observed O₃ concentrations

3.1 Model evaluation

In this section, we evaluate the model's performance by comparing the simulated surface O₃ concentrations with observations from rural/regional background sites and the network of the
25 Chinese National Environmental Monitoring Center (<http://datacenter.mep.gov.cn/>).

For 2003, only a few non-urban sites over CEC have surface O₃ measurements available. We selected six rural/regional background sites for the model evaluation: Mt Tai (36.25 °N, 117.10 °E; 1534 m a.s.l.), Mt Hua (34.49 °N, 110.09 °E; 2064 m a.s.l.), Mt Huang (30.13 °N, 118.15 °E; 1840 m a.s.l.), Shangdianzi (SDZ: 40.65 °N, 117.12 °E; 293 m a.s.l.), Lin'an (30.30 °N, 119.73 °E; 139
30 m a.s.l.), and Hok Tsui (22.22 °N, 114.25 °E; 60 m a.s.l.) (see Fig. S1 for the locations of these



sites). The monthly mean O₃ concentrations at these six sites were taken from the literature (Li et al., 2007; Meng et al., 2009; Wang et al., 2009; Fan et al., 2013; Sun et al., 2016). We compare the simulated surface O₃ concentrations with the 2003 observations for Mt Tai and Hok Tsui but with the 2004 observations for the other four sites.

5 Figure 1(a) compares the observed and simulated monthly mean O₃ concentrations at the six sites. The simulated O₃ concentrations match the observations at Mt Tai, SDZ, and Mt Hua well, with only minor positive biases (1–4 ppbv). In contrast, the model overestimates the O₃ concentrations at Mt Huang, Lin'an, and Hok Tsui by approximately 10 ppbv. These sites in the south sector are often rainy or cloudy during summer, so the overestimation of O₃ is likely to be
10 due to the model's underestimation of precipitation and cloud cover (Ni et al., 2018). The overestimation at the Hok Tsui coastal site of Hong Kong also reflects that the model resolution is insufficient to capture the local terrains and transport pathway (Ni et al., 2018). Similar results were obtained from the comparison between observed and simulated monthly mean O₃ concentrations at the six sites in July 2004 (see Figure S2).

15 For 2015, the simulated O₃ concentrations are compared with observations by the network of the Chinese National Environmental Monitoring Center over East China (Figure 1(b)). To avoid contamination by local pollutants, we select 115 non-urban sites located in 115 cities of East China. For cities in which no non-urban sites are available, we choose sites that are least affected by local pollution (i.e., sites relatively far away from roads, factories, power plants, etc.). For
20 MDA8 O₃, the model results are highly correlated with the observations at most sites ($R^2 = 0.79$). The model only overestimates the monthly MDA8 O₃ by approximately 2.7 ± 5.9 ppbv over CEC.

The model also captures the spatial distribution of MDA8 O₃ very well. It ranges from 40–60 ppbv in the south to 80–100 ppbv in the north of CEC (Figure 2(b)), similar to patterns reported by Lin et al. (2009) and Lou et al. (2015). Hourly O₃ concentrations from the model and
25 observations at Mt Tai in 2003 and nine representative sites in 2015 are compared in Figures S3 and S4, respectively. The model reproduces the diurnal variations in O₃ with a normalised mean bias of 4% at Mt Tai. For the nine sites, the model captures most day-to-day variability (Figure S4). However, it produces larger biases during the night, mostly due to the titration of NO and a lower inversion layer (Yan et al., 2018a). The overestimation of O₃ concentrations in the
30 afternoon is likely to be due to the overestimated precursor emissions in the model.



The observed MDA8 O₃ at SDZ station increased by about 10.8 ppbv from July 2004 to July 2014, comparable to the simulated result, which showed an increase of about 9.5 ppbv from July 2003 to July 2015. In addition, the increasing trend of observed O₃ at Mt Tai was 2.2 ppbv yr⁻¹ from 2003 to 2015, higher than the simulated increase of about 1.3 ppbv yr⁻¹. Nonetheless, the
5 model captures the significant increase in surface O₃ levels over CEC between July 2003 and July 2015.

3.2 Spatial distribution and diurnal variation simulated in different model scenarios

Figure 2 shows the simulated spatial distribution of monthly mean surface MDA8 O₃ over eastern China (100°E to 125°E, 20°N to 50°N) for July 2003 and July 2015. The model simulates
10 relatively high O₃ concentrations over the North China Plain and Sichuan Basin, where anthropogenic emissions of O₃ precursors are high. In July 2003, only a small area in CEC had an MDA8 O₃ concentration exceeding the Level II National Ambient Air Quality Standard (75 ppbv) (Figure 2(a)), but in July 2015 it had expanded to nearly half of this region. The regional mean MDA8 O₃ increased from 65.5±7.9 ppbv in July 2003 to 74.4±8.7 ppbv in July 2015
15 (Table 2). This increasing rate (0.74 ppbv yr⁻¹) is slightly smaller than the findings of most studies (positive trends: 1–3 ppbv yr⁻¹) in this region over the past decade (Ding et al., 2008; Ma et al., 2016; Sun et al., 2016; Xu et al., 2008; Zhang et al., 2014b). Both daily mean and MDA8 O₃ concentrations were significantly higher in July 2015 than in July 2013 over most areas of CEC (Figure 3). As the concentrations of MDA8 O₃ over southwestern China did not exceed the
20 Level II National Ambient Air Quality Standard in July 2015, we do not focus our analysis on this area in the following sections.

The diurnal variation of O₃ over CEC illustrated in Figure 4 shows that O₃ increases by 4.9–6.7 ppbv before dawn (02:00–07:00) and by 8.5–9.0 ppbv in the afternoon (13:00–18:00). The much more significant increase of O₃ in the afternoon in July 2015 is likely to be due to the stronger
25 photochemical production, which is affected by both meteorological conditions and O₃ precursor emissions. The slight increase in night-time O₃ reflects the residual effect of the daytime increase, despite strong night-time titration by NO. This result is very different from the trends over the US, where summertime daytime O₃ increased over the past decades in contrast to the night-time decrease in all seasons (Yan et al., 2018a). Therefore, we focus on the MDA8 O₃ changes over
30 CEC between July 2003 and July 2015.



4. Impacts of meteorology on surface O₃

We performed sensitivity tests to investigate the effects of meteorology and emissions on the MDA8 O₃ over CEC. The contributions of meteorological change to the change in MDA8 O₃ are defined by the 03E15M-03E03M and 15E15M-15E03M simulations. Here we discuss only
5 03E15M-03E03M in detail, as the results of 15E15M-15E03M are similar.

The regional averaged MDA8 O₃ simulated by 03E15M is 68.7 ± 7.1 ppbv, comparable with that simulated by 15E03M (69.6 ± 8.9 ppbv), indicating the comparable contributions made by the changes in meteorology and in emissions. Figure 5 shows the spatial distribution of MDA8 O₃ changes between different simulation scenarios. The domain-averaged MDA8 O₃ is
10 approximately 5.8 ± 3.9 ppbv (5%–95% interval: -0.1 – 12.4 ppbv) higher in scenario 03E15M than in 03E03M (Figure 5(a)) over the central part of CEC (106°E to 115°E , 28°N to 40°N). Over the eastern coastal areas (115°E to 120°E , 28°N to 40°N), however, the MDA8 O₃ in the former scenario is less than in the latter by approximately -0.8 ± 3.5 ppbv (5%–95% interval: -6.8 – 3.8 ppbv), indicating great spatial variation in the influence of meteorological changes.

15 Atmospheric circulation patterns complicate the prediction of O₃ concentrations in a specific region (He et al., 2012). The geopotential height map in Figure S5 shows a high-pressure system over CEC at 850 hPa in July 2015. It is well known that high O₃ pollution events preferentially occur under high-pressure conditions (Wild et al., 2004; Zhao et al., 2009; Xu et al., 2011). This is because the relatively high geopotential height induces a stable weather condition. Neither
20 horizontal nor vertical transport is strong, which favours the accumulation of atmospheric pollutants such as surface O₃. We found that in July 2015, the wind speeds over southern and eastern boundaries of CEC were much slower than that in July 2003 (Figure S6), leading to much lower O₃ flux across these two boundaries. The low O₃ over southern CEC in July 2003 was mainly due to the strong south-westerly wind, decreasing O₃ levels in this area. However, a
25 large amount of O₃ and its precursors from the central part of CEC were transported to the eastern coastal area, which increased O₃ concentrations there (refer to Table 4: about 1343 Gg mon^{-1} O₃ transported out across the east boundary). Conversely, in July 2015, only a small amount of O₃ (refer to Table 4: -61 Gg mon^{-1}) and its precursors were transported away from the ocean by the weak south-easterly winds, which only decreased the O₃ levels in the coastal area.
30 However, in the central part of CEC, the wind was weak, leading to accumulating O₃ pollution in



this area. As a result, the O₃ concentrations increased in the central part of CEC and decreased in the eastern coastal area in July 2015 compared to July 2003.

In addition to the wind, air temperature and relative humidity are two other important meteorological parameters that can affect atmospheric O₃ concentrations. High temperatures tend to accelerate the rate of ozone-related photochemical reactions, promoting O₃ production (Ramsey et al., 2014). Cloud indirectly affects O₃ pollution by blocking solar radiation, thus affecting the emission of BVOCs and the photochemical production of O₃ (Lin et al., 2009). Neither air temperature nor relative humidity plays an important role in explaining the difference in surface O₃ between 2003 and 2015; they are at almost the same levels (Figure S7). The average net production of O₃ over CEC simulated by 03E03M (11.7 ppbv day⁻¹) is very close to that simulated by 03E15M (11.9 ppbv day⁻¹) (Table 4), suggesting that meteorological factors in 2003 and 2015 did not greatly change O₃ photochemical reactions.

Table 2 shows the monthly mean MDA8 O₃ over CEC. We summarise the regional mean O₃ over CEC and regions with MDA8 O₃ >75 ppbv in July 2015. To avoid the influence of uneven spatial distributions of O₃ concentration changes, we performed a gradient analysis. The differences in MDA8 O₃ were analysed in four ways: regional mean, $\Delta\text{MDA8 O}_3 \geq 0$ ppbv (the region over which the difference of MDA8 O₃ between the 2003 standard and 2015 standard simulation (15E15M-03E03M) is positive), $\Delta\text{MDA8 O}_3 \geq 5$ ppbv and $\Delta\text{MDA8 O}_3 \geq 10$ ppbv. For the regional mean over CEC, the increase in O₃ concentration driven by meteorology is approximately 3.1 ± 4.9 ppbv, from 65.5 ± 7.9 ppbv (03E03M) to 68.7 ± 7.1 ppbv (03E15M). Where $\Delta\text{MDA8 O}_3 \geq 10$ ppbv, mostly over the central part of CEC, the O₃ concentration increases by 6.7 ± 3.4 ppbv from 64.3 ± 9.7 ppbv to 71.0 ± 7.4 ppbv due to the meteorological change. Thus, the meteorological conditions have a greater impact on the O₃ change when the difference between 2003 and 2015 is higher than 10 ppbv. Similar results are also found in regions with MDA8 O₃ >75 ppbv, where the increase in the O₃ concentration is approximately 3.6 ± 3.2 ppbv and 5.1 ± 2.5 ppbv for the regional mean and for the $\Delta\text{MDA8 O}_3 \geq 10$ case, respectively. This indicates that surface O₃ levels are more sensitive to meteorological conditions in regions with larger O₃ increase.

5. Impact of emission changes on surface O₃



As described above, the impact of emission changes on MDA8 O₃ concentrations between 2003 and 2015 can be estimated by 15E03M-03E03M or 15E15M-03E15M. Here we discuss only 15E03M-03E03M in detail. Similar results were found from 15E15M-03E15M.

Figure 5(b) shows the contributions of emission changes to surface O₃ levels. The emission change leads to an increase in MDA8 O₃ over most areas of CEC, and it has a much smaller spatial variability than the meteorological change does (Figure 5(a)). Compared to the influence of the meteorological change (03E15M-03E03M: 3.1±4.9 ppbv), the increase in emissions leads to a higher regional mean O₃ increase (15E03M-03E03M: 4.0±1.9 ppbv) over CEC (Table 2). In contrast, for the case of Δ MDA8 O₃ ≥ 10 ppbv, the influence of emission change on O₃ (15E03M-03E03M: 4.5±2.1 ppbv) is smaller than that of the meteorological field change (03E15M-03E03M: 6.7±3.4 ppbv). The increases of MDA8 O₃ due to emission change are about 3.5±1.4 ppbv (5%–95% interval: 1.6–6.0 ppbv) and 5.6±1.8 ppbv (5%–95% interval: 2.2–8.4 ppbv) over the central and eastern parts of CEC, which are different with the spatial pattern caused by meteorological condition change. It is worth noting that in the polluted regions where MDA8 O₃ > 75 ppbv, even if the Δ MDA8 O₃ is greater than 10 ppbv, the O₃ increase caused by emission change is still higher than that caused by meteorological conditions, indicating the dominant effect of emissions on O₃ pollution in the highly polluted regions.

We summarise the emissions of NO_x, CO and NMVOCs over CEC for July 2003 and July 2015 in Table 3. The anthropogenic NO_x emissions increased from 397 Gg mon⁻¹ in July 2003 to 683 Gg mon⁻¹ in July 2015. The anthropogenic NMVOCs also increased significantly, with the NMVOC emissions increasing from 190 Gg C mon⁻¹ in July 2003 to 365 Gg C mon⁻¹ in July 2015. Anthropogenic CO emissions increased from 4619 Gg mon⁻¹ in July 2003 to 6011 Gg mon⁻¹ in July 2015. The natural BVOCs, which are greatly affected by meteorological conditions, remained unchanged between 2003 and 2015. Biomass burning often occurs sequentially from south to north in CEC in the spring harvest season and lasts from late May to mid-June (Chen et al., 2017). In July, the biomass burning emissions generally decrease to approximately 1% of the anthropogenic emissions (not shown). Therefore, the effect of the emission change on O₃ is primarily due to anthropogenic emissions of NO_x and NMVOCs.

To separate the effect of anthropogenic emissions from the effect of natural emission on O₃ variability, we conducted two further simulations, 03N15M and 03V15M (see Section 2.2).



Figure 6 shows the spatial distribution of the MDA8 O₃ differences between the 2015 standard simulation and these two simulations. Anthropogenic NMVOCs (Figure 6 (a)) have a great impact on MDA8 O₃ over the eastern part of CEC, increasing its concentration by approximately 2.5±0.8 ppbv (5%–95% interval: 1.1–3.7 ppbv). The change in O₃ concentrations due to anthropogenic NMVOCs varies from -0.5 ppbv to 5.1 ppbv over different sub-regions of CEC, with a regional mean of 1.4±1.1 ppbv. The effect of anthropogenic NO_x (Figure 6 (b)), in comparison, is more complicated. From 2003 to 2015, MDA8 O₃ declined in some cities such as Tianjin, Ji'nan, Taiyuan, and Nanjing in the eastern part of CEC, but increased in the central and western parts (domain mean: 2.8±0.9 ppbv, 5%–95% interval: 1.4–4.1 ppbv). The change in MDA8 O₃ due to anthropogenic NO_x varies from -3.1 ppbv to 6.7 ppbv, with a regional mean of 2.5±1.1 ppbv over CEC (5%–95% interval: -0.2–3.3 ppbv). The reduction of O₃ in the urban area is likely to be due to the abundant NO_x from industrial and traffic sources. Beijing shows a slight decrease in NO_x and NMVOC emissions, leading to a slight change in O₃ levels. In most rural areas of CEC, O₃ formation tends to be limited by the concentrations of NO_x (the so-called NO_x-limited regime). Thus, O₃ is increased significantly as we increase the anthropogenic emissions of NO_x. A VOC-limited regime in a few urban areas and a NO_x-limited/transition regime in regional rural areas of CEC have been reported in some observational and model simulation studies (Wang et al., 2017 and references therein). The change in BVOC emissions only leads to a small change in MDA8 O₃ over CEC, resulting in an increase in the O₃ level of only 0.3 ppbv (not shown), mostly due to the change in meteorological conditions. Therefore, if the meteorological conditions are fixed as the 2015 conditions, the increase in anthropogenic NMVOCs is the most important factor responsible for the in O₃ increase over the eastern part of CEC, whereas NO_x emissions tend to increase O₃ concentrations over central and western parts but decrease it in a few urban areas over eastern parts of CEC.

6. Process analyses

Ozone concentrations are determined by chemical and dynamic processes including transport, chemical production and loss, and deposition. In this section, we discuss the effect of these processes on the surface O₃ over CEC.

Table 4 documents the horizontal and vertical mass fluxes of O₃ over CEC at four boundaries (north, east, south and west). The flux at each boundary was calculated from surface to 850 hPa.



In July 2003, the air flows into CEC through the south boundary, and then out across the other three boundaries. In contrast, the air masses flow into this area across the east boundary in July 2015, and then out across the left three boundaries. The larger O₃ flux from each boundary in July 2003 is due to stronger winds. Compared to the 03E03M simulation (-897 Gg mon⁻¹; minus value means export of O₃ from this region), 03E15M shows a much lower O₃ flux (-401 Gg mon⁻¹), indicating that weather conditions in 2015 play a more important role in pollutant accumulation, which is consistent with our analysis in Section 4. The larger O₃ flux in 15E03M (-1232 Gg mon⁻¹) in comparison to the 03E03M simulation, however, is mostly due to the increased precursor emissions in 2015.

Table 4 also shows the chemical production and loss of O₃ over CEC from surface to 850 hPa. The net photochemical production of O₃ in July 2015 (2158 Gg mon⁻¹ or 15.5 ppbv day⁻¹) is higher than that in July 2003 (1629 Gg mon⁻¹ or 11.7 ppbv day⁻¹). By comparing the 03E03M simulation with 03E15M simulation, we find that the weather conditions in 2015 do not promote excessive O₃ production (03E15M: 1657 Gg mon⁻¹ or 11.9 ppbv day⁻¹), almost the same level as 03E03M simulation. In comparison, due to more O₃ precursor emissions in 2015, the O₃ production by 15E03M (2166 Gg mon⁻¹ or 15.6 ppbv day⁻¹) is much higher than the 03E03M simulation. The net photochemical O₃ production in this study is similar to the result of Li et al. (2007), who reported a net production of 10–32 ppbv day⁻¹ at three mountain sites over CEC in 2004. Deposition (mainly dry deposition) is another factor that affects O₃ concentrations. The 03E15M simulation shows an increase in O₃ dry deposition by only 10 Gg mon⁻¹, compared to the 03E03M simulation (156 Gg mon⁻¹). So dry deposition is less affected by changes in weather conditions.

As shown in Table 4, the O₃ budget analysis indicates CEC is a strong photochemical source region in both 2003 and 2015. The photochemically produced O₃ is exported by transport and to a lesser extent removed by dry deposition. In July 2003, about half of photochemically formed O₃ in the CEC region was removed by transport in July 2015. Comparing the results of the 2003 and 2015 standard simulations (15E15M-03E03M), we find that the absolute value of O₃ transport flux increased by 395 Gg mon⁻¹ (2015-2003), net O₃ production increased by 529 Gg mon⁻¹ and O₃ dry deposition only increased by 24 Gg mon⁻¹. As a result, the increase in O₃ concentrations from July 2003 to July 2015 is mainly due to transboundary horizontal transport, vertical transport and photochemical reactions.



7. Conclusions

In this study, we used the global GEOS-Chem model and its Asia nested model to simulate surface O_3 over Central Eastern China between July 2003 and July 2015. We found that the regional averaged concentration of MDA8 O_3 increased from 65.5 ± 7.9 ppbv in 2003 to 74.4 ± 8.7 ppbv in 2015. The increase in the regional average MDA8 O_3 due to emission changes (4.0 ± 1.9 ppbv) is higher than that caused by meteorological changes (3.1 ± 4.9 ppbv) compared with the 2003 standard simulation. The effects of meteorological changes have a larger spatial variability than those of emission changes. The increase in anthropogenic NMVOC emissions increased O_3 concentrations over the eastern part of CEC, whereas the increased anthropogenic NO_x emissions dominated the increase in O_3 over the central and western parts of CEC but decreased O_3 levels in a few urban areas over eastern CEC. The O_3 formation over most areas is in NO_x -limited or transition regime, whereas a few urban areas tend to be in VOC-limited regime. The increase in surface O_3 concentrations is mainly via photochemical production and transport processes. The transport pattern in July 2015 tends to enhance O_3 levels over the central part of CEC, while the meteorological condition in 2015 does not promote the O_3 production. The increased net O_3 photochemical production is mostly due to increased precursor emissions.

Our results have implications for the formulation of effective control strategies for O_3 air pollution in CEC. Although the simulated average effect of emission changes is larger than the effect of meteorological changes, the regions with larger O_3 increases (e.g., $\Delta MDA8 O_3 \geq 10$ ppbv) show a higher sensitivity to meteorology than to emission changes. The results imply that assessment of the effectiveness of regional and urban O_3 control strategies needs to be placed in the context of meteorology. The O_3 transport flux analysis further suggests that large-scale regional transport is an important contributor to the surface O_3 increases from 2003 to 2015. Transboundary transport issues in local O_3 control strategies should go beyond transport from neighbouring areas and account for long-distance transport, particularly in the context of globalizing air pollution.

Acknowledgements

This research was supported by the National Key Research and Development Program of China (2016YFC0200500), the National Natural Science Foundation of China (41675118, 91544213, 41775115), the Qilu Youth Talent Program of Shandong University, the Jiangsu



Collaborative Innovation Center for Climate Change, and the Taishan Scholars (ts201712003). The model simulations were done at the Supercomputing Center of Shandong University in Weihai. We thank the Chinese National Environmental Monitoring Center for providing the observation data. Lei Sun acknowledges the support of the China Scholarship Council.

5 References

- Auvray, M., and Bey, I.: Long-range transport to Europe: Seasonal variations and implications for the European ozone budget, *J. Geophys. Res.-Atmos.*, 110, D11303, <https://doi.org/10.1029/2004JD005503>, 2005.
- Chen, J., Li, C., Ristovski, Z., Milic, A., Gu, Y., Islam, M. S., Wang, S., Hao, J., Zhang, H., He, C., Guo, H., Fu, H., Miljevic, B., Morawska, L., Thai, P., Fat, L., Pereira, G., Ding, A., Huang, X., and Dumka, U.: A review of biomass burning: Emissions and impacts on air quality, health and climate in China, *Sci. Total Environ.*, 579, 1000-1034, <https://doi.org/10.1016/j.scitotenv.2016.11.025>, 2017.
- China State Council: Twelfth Five-Year Plan on National Economy and Social Development of the People's Republic of China, available at: http://www.gov.cn/2011lh/content_1825838.htm, 2011 (in Chinese).
- Cooper, O. R., Gao, R. S., Tarasick, D., Leblanc, T., and Sweeney, C.: Long-term ozone trends at rural ozone monitoring sites across the United States, 1990–2010, *J. Geophys. Res.-Atmos.*, 117, D22307, <https://doi.org/10.1029/2012JD018261>, 2012.
- Cooper, O. R., Parrish, D., Ziemke, J., Balashov, N., Cupeiro, M., Galbally, I., Gilge, S., Horowitz, L., Jensen, N., Lamarque, J.-F., Naik, V., Oltmans, S., Schwab, J., Shindell, D., Thompson, A., Thouret, V., Wang, Y., and Zbinden, R.: Global distribution and trends of tropospheric ozone: An observation-based review, *Elem. Sci. Anth.*, 2:29, <http://doi.org/10.12952/journal.elementa.000029>, 2014.
- Crutzen, P.: A discussion of the chemistry of some minor constituents in the stratosphere and troposphere, *Pure Appl. Geophys.*, 106, 1385-1399, <https://doi.org/10.1007/BF00881092>, 1973.
- Danielsen, E. F.: Stratospheric-tropospheric exchange based on radioactivity, ozone and potential vorticity, *J. Atmos. Sci.*, 25, 502-518, [https://doi.org/10.1175/1520-0469\(1968\)025<0502:STEBOR>2.0.CO;2](https://doi.org/10.1175/1520-0469(1968)025<0502:STEBOR>2.0.CO;2), 1968.
- Ding, A. J., Wang, T., Thouret, V., Cammas, J. P., and Nédélec, P.: Tropospheric ozone



- climatology over Beijing: Analysis of aircraft data from the MOZAIC program, *Atmos. Chem. Phys.*, 8, 1-13, <https://doi.org/10.5194/acp-8-1-2008>, 2008.
- Fan, Y., Fan, S. Zhang, H, Zu, F., Meng., Q, He, J.: Characteristics of SO₂, NO₂, O₃ volume fractions and their relationship with weather conditions at Linan in summer and winter. *Trans. Atmos. Sci.*, 36 (1): 121-128, , 10.13878/j.cnki.dqkxxb.2013.01.013, (in Chinese), 2013.
- 5 Fu, Y., and Liao, H.: Simulation of the interannual variations of biogenic emissions of volatile organic compounds in China: Impacts on tropospheric ozone and secondary organic aerosol, *Atmos. Environ.*, 59, 170-185, <https://doi.org/10.1016/j.atmosenv.2012.05.053>, 2012.
- Guenther, A., Jiang, X., Heald, C., Sakulyanontvittaya, T., Duhl, T., Emmons, L., and Wang, X.:
10 The model of emissions of gases and aerosols from nature version 2.1 (MEGAN2. 1): An extended and updated framework for modeling biogenic emissions, *Geosci. Model Dev.*, 5, 1471-1492, <http://hdl.handle.net/1721.1/78869>, 2012.
- He, J., Wang, Y., Hao, J., Shen, L., and Wang, L.: Variations of surface O₃ in August at a rural site near Shanghai: Influences from the West Pacific subtropical high and anthropogenic
15 emissions, *Environ. Sci. Pollut. Res.*, 19, 4016-4029, <https://doi.org/10.1007/s11356-012-0970-5>, 2012.
- He, Y. J., Uno, I., Wang, Z. F., Pochanart, P., Li, J., and Akimoto, H.: Significant impact of the East Asia monsoon on ozone seasonal behavior in the boundary layer of Eastern China and the west Pacific region, *Atmos. Chem. Phys.*, 8, 7543-7555,
20 <https://doi.org/10.5194/acp-8-7543-2008>, 2008.
- Hess, P., and Zbinden, R.: Stratospheric impact on tropospheric ozone variability and trends: 1990–2009, *Atmos. Chem. Phys.*, 13, 649-674, <https://doi.org/10.5194/acp-13-649-2013>, 2013.
- Holtslag, A. A. M., and Boville, B. A.: Local versus nonlocal boundary-layer diffusion in a
25 global climate model, *J. Clim.*, 6, 1825-1842, [https://doi.org/10.1175/1520-0442\(1993\)006<1825:LVNBLD>2.0.CO;2](https://doi.org/10.1175/1520-0442(1993)006<1825:LVNBLD>2.0.CO;2), 1993.
- Hudman, R., Moore, N., Mebust, A., Martin, R., Russell, A., Valin, L., and Cohen, R.: Steps towards a mechanistic model of global soil nitric oxide emissions: Implementation and space based-constraints, *Atmos. Chem. Phys.*, 12, 7779-7795,
30 <https://doi.org/10.5194/acp-12-7779-2012>, 2012.
- IPCC: Climate change 2013: The physical science basis. In: Stocker, T.F., et al. (Eds.),



- Contribution of Working Group I to the Fifth Assessment Report of the Intergovernmental Panel on Climate Change. Cambridge University Press, Cambridge, United Kingdom and New York, 1-1535., 2013.
- Jacob, D. J., Logan, J. A., and Murti, P. P.: Effect of rising Asian emissions on surface ozone in
5 the United States, *Geophys. Res. Lett.*, 26, 2175-2178, <https://doi.org/10.1029/1999GL900450>, 1999.
- Kuhns, H., Green, M., Etyemezian, V., Watson, J., and Pitchford, M.: Big Bend Regional Aerosol and Visibility Observational (BRAVO) Study Emissions Inventory, Report prepared for BRAVO Steering Committee, Desert Research Institute, Las Vegas, Nevada, 2003.
- 10 Kurokawa, J., Ohara, T., Morikawa, T., Hanayama, S., Janssens-Maenhout, G., Fukui, T., Kawashima, K., and Akimoto, H.: Emissions of air pollutants and greenhouse gases over Asian regions during 2000–2008: Regional Emission inventory in ASia (REAS) version 2, *Atmos. Chem. Phys.*, 13, 11019-11058, <https://doi.org/10.5194/acp-13-11019-2013>, 2013.
- Li, J., Wang, Z., Akimoto, H., Gao, C., Pochanart, P., and Wang, X.: Modeling study of ozone
15 seasonal cycle in lower troposphere over east Asia, *J. Geophys. Res.-Atmos.*, 112, D22S25, <https://doi.org/10.1029/2006JD008209>, 2007.
- Li, M., Liu, H., Geng, G., Hong, C., Liu, F., Song, Y., Tong, D., Zheng, B., Cui, H., Man, H., Zhang, Q., and He, K.: Anthropogenic emission inventories in China: A review, *Natl. Sci. Rev.*, <https://doi.org/10.1093/nsr/nwx150>, 2017a.
- 20 Li, M., Zhang, Q., Kurokawa, J.-i., Woo, J.-H., He, K., Lu, Z., Ohara, T., Song, Y., Streets, D. G., Carmichael, G. R., Cheng, Y., Hong, C., Huo, H., Jiang, X., Kang, S., Liu, F., Su, H., and Zheng, B.: MIX: A mosaic Asian anthropogenic emission inventory under the international collaboration framework of the MICS-Asia and HTAP, *Atmos. Chem. Phys.*, 17, 935-963, <https://doi.org/10.5194/acp-17-935-2017>, 2017b.
- 25 Lin, J. T., Wuebbles, D. J., and Liang, X. Z.: Effects of intercontinental transport on surface ozone over the United States: Present and future assessment with a global model, *Geophys. Res. Lett.*, 35, L02805, <https://doi.org/10.1029/2007GL031415>, 2008.
- Lin, M., Holloway, T., Oki, T., Streets, D., and Richter, A.: Multi-scale model analysis of boundary layer ozone over East Asia, *Atmos. Chem. Phys.*, 9, 3277-3301,
30 <https://doi.org/10.5194/acp-9-3277-2009>, 2009.
- Lin, M., Fiore, A. M., Horowitz, L. W., Langford, A. O., Oltmans, S. J., Tarasick, D., and Rieder,



- H. E.: Climate variability modulates western US ozone air quality in spring via deep stratospheric intrusions, *Nat. Commun.*, 6, 7105, <https://doi.org/10.1038/ncomms8105>, 2015.
- Logan, J. A.: Tropospheric ozone: Seasonal behavior, trends, and anthropogenic influence, *J. Geophys. Res.-Atmos.*, 90, 10463-10482, <https://doi.org/10.1029/JD090iD06p10463>, 1985.
- 5 Lou, S., Liao, H., Yang, Y., and Mu, Q.: Simulation of the interannual variations of tropospheric ozone over China: Roles of variations in meteorological parameters and anthropogenic emissions, *Atmos. Environ.*, 122, 839-851, <https://doi.org/10.1016/j.atmosenv.2015.08.081>, 2015.
- Ma, Z., Xu, J., Quan, W., Zhang, Z., Lin, W., and Xu, X.: Significant increase of surface ozone at a rural site, north of eastern China, *Atmos. Chem. Phys.*, 16, 3969-3977, <https://doi.org/10.5194/acp-16-3969-2016>, 2016.
- 10 Mao, J., Paulot, F., Jacob, D. J., Cohen, R. C., Crouse, J. D., Wennberg, P. O., Keller, C. A., Hudman, R. C., Barkley, M. P., and Horowitz, L. W.: Ozone and organic nitrates over the eastern United States: Sensitivity to isoprene chemistry, *J. Geophys. Res.-Atmos.*, 118, 11256-11268, <https://doi.org/10.1002/jgrd.50817>, 2013.
- McLinden, C. A., S. C. Olsen, B. Hannegan, O. Wild, M. J. Prather, and J. Sundet: Stratospheric ozone in 3-D models: A simple chemistry and the cross-tropopause flux, *J. Geophys. Res.-Atmos.*, 105, 14653-14665, <https://doi.org/10.1029/2000JD900124>, 2000.
- Meng, Z., Xu, X., Yan, P., Ding, G., Tang, J., Lin, W., Xu, X., and Wang, S.: Characteristics of trace gaseous pollutants at a regional background station in Northern China, *Atmos. Chem. Phys.*, 9, 927-936, <https://doi.org/10.5194/acp-9-927-2009>, 2009.
- 20 Monks, P. S.: A review of the observations and origins of the spring ozone maximum, *Atmos. Environ.*, 34, 3545-3561, [https://doi.org/10.1016/S1352-2310\(00\)00129-1](https://doi.org/10.1016/S1352-2310(00)00129-1), 2000.
- Monks, P. S., Archibald, A. T., Colette, A., Cooper, O., Coyle, M., Derwent, R., Fowler, D., Granier, C., Law, K. S., Mills, G. E., Stevenson, D. S., Tarasova, O., Thouret, V., von Schneidmesser, E., Sommariva, R., Wild, O., and Williams, M. L.: Tropospheric ozone and its precursors from the urban to the global scale from air quality to short-lived climate forcer, *Atmos. Chem. Phys.*, 15, 8889-8973, <https://doi.org/10.5194/acp-15-8889-2015>, 2015.
- 25 Murray, L. T., Jacob, D. J., Logan, J. A., Hudman, R. C., and Koshak, W. J.: Optimized regional and interannual variability of lightning in a global chemical transport model constrained by LIS/OTD satellite data, *J. Geophys. Res.-Atmos.*, 117, D20307
- 30



<https://doi.org/10.1029/2012JD017934>, 2012.

Ni, R., Lin, J., Yan, Y., Lin W. Foreign and domestic contributions to springtime ozone over China. *Atmos. Chem. Phys. Discuss.*, <https://doi.org/10.5194/acp-2017-1226>, 2018.

Oltmans, S. J., Lefohn, A. S., Shadwick, D., Harris, J. M., Scheel, H. E., Galbally, I., Tarasick, D.,
5 W., Johnson, B. J., Brunke, E. G., Claude, H., Zeng, G., Nichol, S., Schmidlin, F., Davies, J.,
Cuevas, E., Redondas, A., Naoe, H., Nakano, T., and Kawasato, T.: Recent tropospheric ozone
changes: A pattern dominated by slow or no growth, *Atmos. Environ.*, 67, 331-351,
<https://doi.org/10.1016/j.atmosenv.2012.10.057>, 2013.

Ott, L. E., Pickering, K. E., Stenchikov, G. L., Allen, D. J., DeCaria, A. J., Ridley, B., Lin, R. F.,
10 Lang, S., and Tao, W. K.: Production of lightning NO_x and its vertical distribution calculated
from three-dimensional cloud-scale chemical transport model simulations, *J. Geophys.
Res.-Atmos.*, 115, D04301, <https://doi.org/10.1029/2009JD011880>, 2010.

Parrish, D., Lamarque, J. F., Naik, V., Horowitz, L., Shindell, D., Staehelin, J., Derwent, R.,
Cooper, O., Tanimoto, H., Volz-Thomas, A., Gilge, S., Scheel, H.-E., Steinbacher, M., and
15 Fröhlich, M.: Long-term changes in lower tropospheric baseline ozone concentrations:
Comparing chemistry-climate models and observations at northern midlatitudes, *J. Geophys.
Res.-Atmos.*, 119, 5719-5736, <https://doi.org/10.1002/2013JD021435>, 2014.

Price, C., and Rind, D.: A simple lightning parameterization for calculating global lightning
distributions, *J. Geophys. Res.-Atmos.*, 97, 9919-9933, <https://doi.org/10.1029/92JD00719>,
20 1992.

Ramsey, N. R., Klein, P. M., and Moore, B.: The impact of meteorological parameters on urban
air quality, *Atmos. Environ.*, 86, 58-67, <https://doi.org/10.1016/j.atmosenv.2013.12.006>, 2014.

Randerson, J., Chen, Y., Werf, G., Rogers, B., and Morton, D.: Global burned area and biomass
burning emissions from small fires, *J. Geophys. Res.*, 117, G04012,
25 <https://doi.org/10.1029/2012JG002128>, 2012.

Real, E., Law, K. S., Weinzierl, B., Fiebig, M., Petzold, A., Wild, O., Methven, J., Arnold, S.,
Stohl, A., Huntrieser, H., Roiger, A., Schlager, H., Stewart, D., Avery, M., Sachse, G., Browell,
E., Ferrare, R., and Blake, D.: Processes influencing ozone levels in Alaskan forest fire plumes
during long-range transport over the North Atlantic, *J. Geophys. Res.-Atmos.*, 112, D10S41,
30 <https://doi.org/10.1029/2006JD007576>, 2007.

Seinfeld, J. H., and Pandis, S. N.: *Atmospheric Chemistry and Physics: From Air Pollution to*



- Climate Change, John Wiley & Sons, 2016.
- Sun, L., Xue, L., Wang, T., Gao, J., Ding, A., Cooper, O. R., Lin, M., Xu, P., Wang, Z., Wang, X.,
Wen, L., Zhu, Y., Chen, T., Yang, L., Wang, Y., Chen, J., and Wang, W.: Significant increase of
summertime ozone at Mount Tai in Central Eastern China, *Atmos. Chem. Phys.*, 16,
5 10637-10650, <https://doi.org/10.5194/acp-16-10637-2016>, 2016.
- Verstraeten, W. W., Neu, J. L., Williams, J. E., Bowman, K. W., Worden, J. R., and Boersma, K.
F.: Rapid increases in tropospheric ozone production and export from China, *Nat. Geosci.*, 8,
690, <https://doi.org/10.1038/ngeo2493>, 2015.
- Wang, T., Ding, A., Gao, J., and Wu, W. S.: Strong ozone production in urban plumes from
10 Beijing, China, *Geophys. Res. Lett.*, 33, L21806, <https://doi.org/10.1029/2006GL027689>,
2006.
- Wang, T., Wei, X., Ding, A., Poon, S. C., Lam, K., Li, Y., Chan, L., and Anson, M.: Increasing
surface ozone concentrations in the background atmosphere of Southern China, 1994-2007,
Atmos. Chem. Phys., 9, 6217-6227, <https://doi.org/10.5194/acp-9-6217-2009>, 2009.
- 15 Wang, T., Xue, L., Brimblecombe, P., Lam, Y. F., Li, L., and Zhang, L.: Ozone pollution in China:
A review of concentrations, meteorological influences, chemical precursors, and effects, *Sci.
Total Environ.*, 575, 1582-1596, <https://doi.org/10.1016/j.scitotenv.2016.10.081>, 2017.
- Wang, Y., Zhang, Y., Hao, J., and Luo, M.: Seasonal and spatial variability of surface ozone over
China: Contributions from background and domestic pollution, *Atmos. Chem. Phys.*, 11,
20 3511-3525, <https://doi.org/10.5194/acp-11-3511-2011>, 2011.
- Wild, O., Pochanart, P., and Akimoto, H.: Trans-Eurasian transport of ozone and its precursors, *J.
Geophys. Res.-Atmos.*, 109, D11302, <https://doi.org/10.1029/2003JD004501>, 2004.
- Xiao, Y., Logan, J. A., Jacob, D. J., Hudman, R. C., Yantosca, R., and Blake, D. R.: Global
budget of ethane and regional constraints on US sources, *J. Geophys. Res.-Atmos.*, 113,
25 D21306, <https://doi.org/10.1029/2007JD009415>, 2008.
- Xu, W., Zhao, C., Ran, L., Deng, Z., Liu, P., Ma, N., Lin, W., Xu, X., Yan, P., He, X., Yu, J.,
Liang, W. D., and Chen, L. L.: Characteristics of pollutants and their correlation to
meteorological conditions at a suburban site in the North China Plain, *Atmos. Chem. Phys.*, 11,
4353-4369, <https://doi.org/10.5194/acp-11-4353-2011>, 2011.
- 30 Xu, X., Lin, W., Wang, T., Yan, P., Tang, J., Meng, Z., and Wang, Y.: Long-term trend of surface
ozone at a regional background station in eastern China 1991–2006: enhanced variability,



- Atmos. Chem. Phys., 8, 2595-2607, <https://doi.org/10.5194/acp-8-2595-2008>, 2008.
- Xue, L., Wang, T., Gao, J., Ding, A., Zhou, X., Blake, D., Wang, X., Saunders, S., Fan, S., Zuo, H., Zhang, Q., and Wang W.: Ground-level ozone in four Chinese cities: Precursors, regional transport and heterogeneous processes, Atmos. Chem. Phys., 14, 13175-13188, <https://doi.org/10.5194/acp-14-13175-2014>, 2014.
- 5 Yamaji, K., Li, J., Uno, I., Kanaya, Y., Irie, H., Takigawa, M., Komazaki, Y., Pochanart, P., Liu, Y., Tanimoto, H., Ohara, T., Yan, X., Wang, Z., and Akimoto, H.: Impact of open crop residual burning on air quality over Central Eastern China during the Mount Tai Experiment 2006 (MTX2006), Atmos. Chem. Phys., 10, 7353-7368, <https://doi.org/10.5194/acp-10-7353-2010>, 2010.
- 10 Yan, Y., Lin, J., and He, C.: Ozone trends over the United States at different times of day, Atmos. Chem. Phys., 18, 1185-1202, <https://doi.org/10.5194/acp-18-1185-2018>, 2018a.
- Yan, Y., Pozzer, A., Ojha, N., Lin, J., and Lelieveld, J.: Analysis of European ozone trends in the period 1995–2014, Atmos. Chem. Phys., 18, 5589-5605, doi.org/10.5194/acp-18-5589-2018, 2018b.
- 15 Zhang, L., Jacob, D. J., Yue, X., Downey, N. V., Wood, D. A., and Blewitt, D.: Sources contributing to background surface ozone in the US Intermountain West, Atmos. Chem. Phys., 14, 5295-5309, <https://doi.org/10.5194/acp-14-5295-2014>, 2014a.
- Zhang, Q., Yuan, B., Shao, M., Wang, X., Lu, S., Lu, K., Wang, M., Chen, L., Chang, C.-C., and Liu, S. C.: Variations of ground-level O₃ and its precursors in Beijing in summertime between 2005 and 2011, Atmos. Chem. Phys., 14, 6089-6101, <https://doi.org/10.5194/acp-14-6089-2014>, 2014b.
- 20 Zhao, C., Wang, Y., and Zeng, T.: East China Plains: A ‘basin’ of ozone pollution, Environ. Sci. Technol., 43, 1911-1915, Doi: 10.1021/es8027764, 2009.
- 25 Zhao, C., Wang, Y., Yang, Q., Fu, R., Cunnold, D., and Choi, Y.: Impact of East Asian summer monsoon on the air quality over China: View from space, J. Geophys. Res.-Atmos., 115, D09301, <https://doi.org/10.1029/2009JD012745>, 2010.
- Zheng, B., Tong, D., Li, M., Liu, F., Hong, C., Geng, G., Li, H., Li, X., Peng, L., Qi, J., Yan, L., Zhang, Y., Zhao, H., Zheng, Y., He, K., and Zhang, Q.: Trends in China's anthropogenic emissions since 2010 as the consequence of clean air actions, Atmos. Chem. Phys. Discuss., <https://doi.org/10.5194/acp-2018-374>, 2018.
- 30

**Table 1.** Model simulation scenarios in this study.

Name	Description
1. 2003 standard (03E03M)	The standard simulation of O ₃ concentrations over China based on 2003 emissions and 2003 meteorology
2. 2015 standard (15E15M)	The standard simulation of O ₃ concentrations over China based on 2015 emissions and 2015 meteorology
3. 03E15M	Same as 2 but with 2003 emissions
4. 15E03M	Same as 2 but with 2003 meteorology
5. 03N15M	Same as 2 but with 2003 anthropogenic NO _x emissions in China
6. 03V15M	Same as 2 but with 2003 anthropogenic NMVOC emissions in China

5 **Table 2.** Monthly mean (standard deviation) MDA8 O₃ over CEC based on four model simulations. Δ MDA8 O₃ represents the difference in O₃ concentrations between the 2015 standard simulation and 2003 standard simulation: Δ MDA8 O₃ = MDA8 O₃ (2015) - MDA8 O₃ (2003). MDA8 O₃ > 75 ppbv indicates the region of MDA8 O₃ exceeding the Level II National Ambient Air Quality Standard (75 ppbv) in July 2015.

10

Region	Description	03E03M	03E15M	15E03M	15E15M
CEC	regional mean	65.5 (7.9)	68.7 (7.1)	69.6 (8.9)	74.4 (8.7)
	Δ MDA8 O ₃ \geq 0	65.6 (8.2)	69.4 (6.9)	69.8 (9.1)	75.6 (8.2)
	Δ MDA8 O ₃ \geq 5.0	65.6 (8.7)	70.6 (6.7)	70.0 (9.7)	77.4 (7.7)
	Δ MDA8 O ₃ \geq 10	64.3 (9.7)	71.0 (7.4)	68.8 (10.8)	78.0 (8.4)
Region with MDA8 O ₃ > 75 ppbv	regional mean	71.0 (4.5)	74.7 (4.2)	76.0 (5.2)	82.2 (4.7)
	Δ MDA8 O ₃ \geq 0	71.0 (4.5)	74.7 (4.2)	76.0 (5.2)	82.2 (4.7)
	Δ MDA8 O ₃ \geq 5.0	70.9 (4.5)	74.7 (4.2)	75.9 (5.3)	82.3 (4.7)
	Δ MDA8 O ₃ \geq 10	70.5 (4.8)	75.5 (4.5)	75.7 (5.6)	83.4 (4.8)



Table 3. Emissions of NO_x, CO and NMVOCs in CEC for July 2003 and July 2015, including anthropogenic emissions and biogenic emissions. Units: NO, CO and CH₂O: Gg mon⁻¹; others: Gg C mon⁻¹.

Species	2003	2015	Species	2003	2015
Anthropogenic emissions					
NO	397	683	Acetaldehyde	2.7	3.0
CO	4619	6011	PRPE ^b	39	70
ALK4 ^a	81	184	C ₃ H ₈	35	56
Acetone	4.2	9.9	CH ₂ O	6.4	7.4
Methyl Ethyl Ketone	1.2	3.6	C ₂ H ₆	21	32
Biogenic emissions					
Isoprene	276	275	b-Pinene	18.4	17.4
Acetone	23.0	22.0	3-Carene	15.3	14.3
PRPE	21.0	21.0	Ocimene	7.3	7.1
a-Pinene	25.9	23.8	Acetaldehyde	10.0	9.0
Total monoterpenes	90	85	Other monoterpenes	11.0	11.0

5 ^a:ALK4: Alkanes and other non-aromatic compounds that react only with OH, and have k_{OH} between 5×10^3 and 1×10^4 ppm⁻¹ min⁻¹.

^b:PRPE: OLE1+OLE2, OLE1: Alkenes (other than ethene) with $k_{OH} < 7 \times 10^4$ ppm⁻¹ min⁻¹; OLE2: Alkenes with $k_{OH} > 7 \times 10^4$ ppm⁻¹ min⁻¹.

10

Table 4. Horizontal and vertical flux (Gg mon⁻¹), photochemical production and loss (Gg mon⁻¹ (ppbv day⁻¹)), and dry deposition (Gg mon⁻¹) of O₃ over CEC from surface to 850 hPa based on four types of simulations. For horizontal flux, positive values indicate eastward or northward transport. For vertical fluxes, positive values indicate upward transport. Net photochemical O₃ production is the difference between production and loss of O₃.

15

Processes	Boundary	03E03M	03E15M	15E03M	15E15M	
Transport	105 E	-176	-145	-190	-149	
	Horizontal	122 E	1343	-129	1450	-61
		28 N	1914	-100	1906	-178
	41 N	440	327	488	351	
	Vertical	850 hPa	852	-43	877	-116
Total		-897	-401	-1100	-502	
Photochemical	Production	2850 (20.5)	2890 (20.7)	3511 (25.2)	3532 (25.4)	
	Loss	1221 (8.8)	1232 (8.9)	1344 (9.7)	1373 (9.9)	
	Net	1629 (11.7)	1657 (11.9)	2166 (15.6)	2158 (15.5)	
Dry deposition		156	166	162	180	

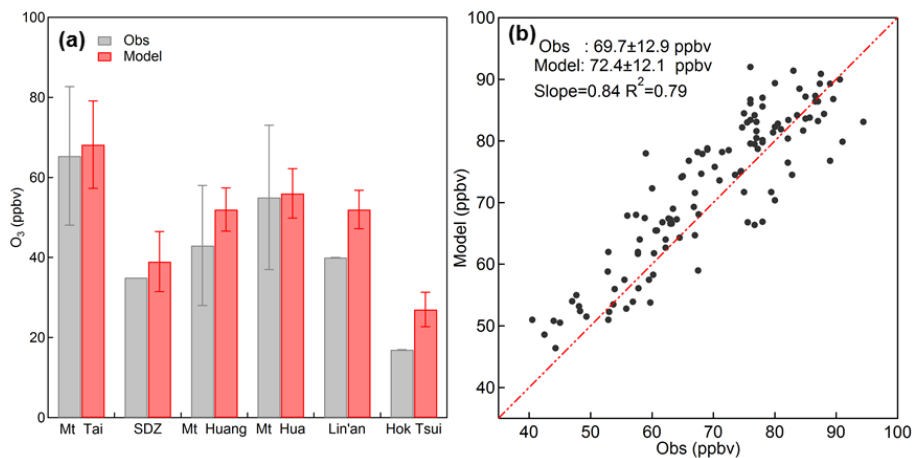


Figure 1. (a) Comparison of observed and simulated monthly mean concentrations of surface O₃ in July 2003. (Mt Tai: July 2003; SDZ: Shangdianzi station: July 2004; Mt Huang: July 2004; Mt Hua: July 2004; Lin'an: July 2004 and Hok Tsui: July 2003). (b) Correlation between observed and modelled monthly mean MDA8 O₃ in July 2015 at 115 stations in Eastern China.

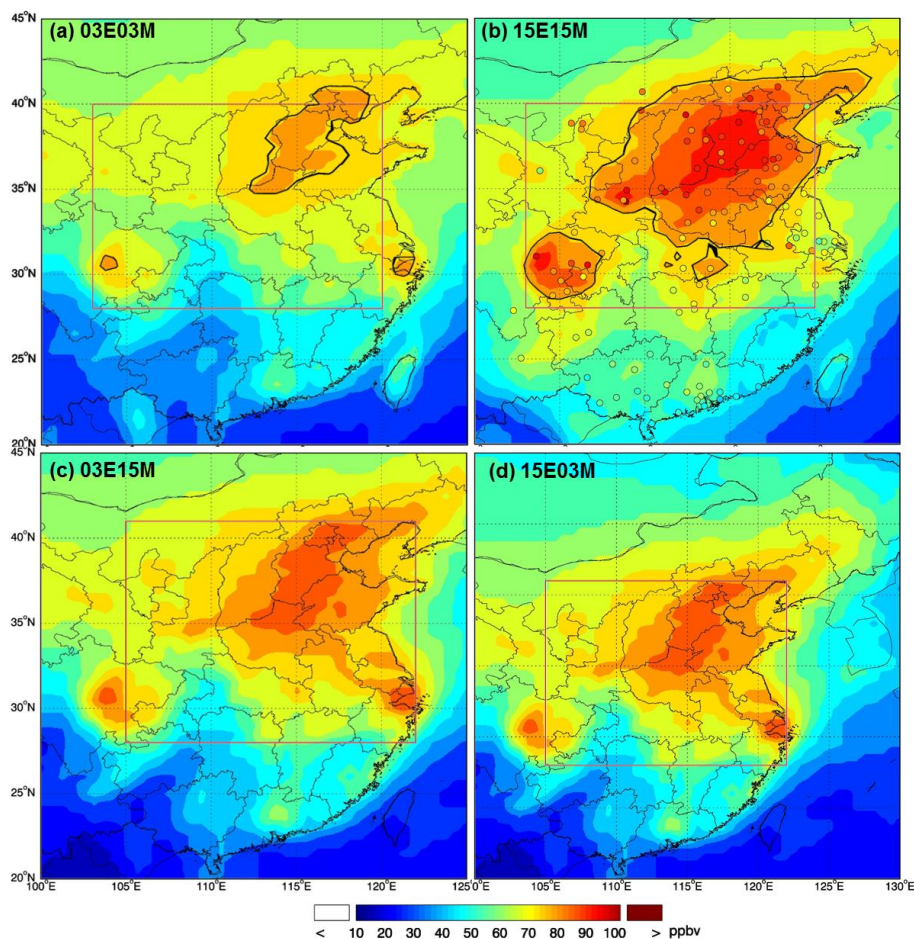


Figure 2. Monthly mean spatial distributions of surface MDA8 O₃ in July over East China. (a) 03E03M: 2003 standard simulation; (b) 15E15M: 2015 standard simulation; (c) 03E15M: 2003 emission + 2015 meteorology and (d) 15E03M: 2015 emission + 2003 meteorology. Black contours in (a) and (b) indicate the regions with MDA8 O₃ > 75 ppbv. Filled circles in (b) show the observed MDA8 O₃ at 115 sites of the network of Chinese National Environmental Monitoring Center. The red rectangle represents the Central Eastern China region (CEC: 103°E-120°E, 28°N-40°N).

5
10

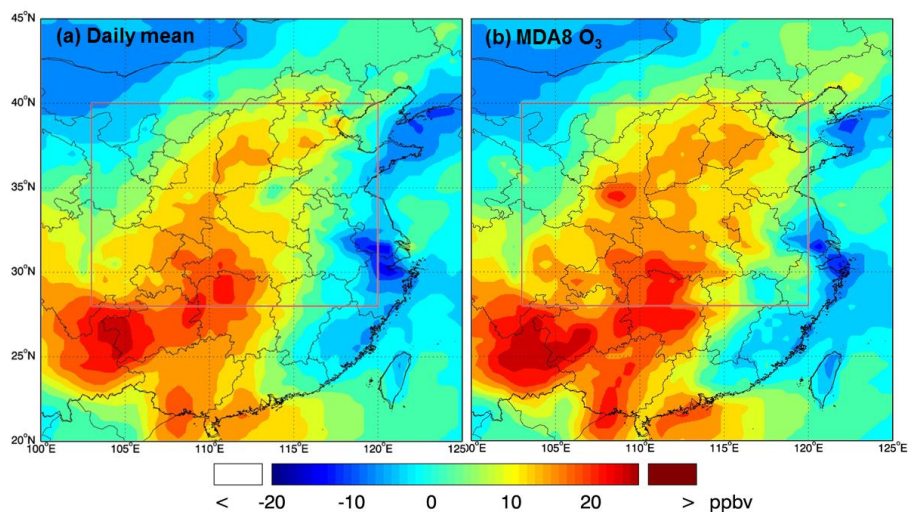


Figure 3. Differences in monthly mean surface O_3 in July of 2003 and 2015 (2015-2003) for daily mean O_3 (a) and MDA8 O_3 (b) simulated by 2003 and 2015 standard simulations.

5

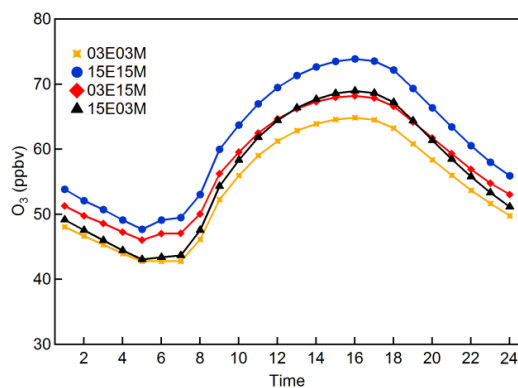


Figure 4. Averaged diurnal variations of surface O_3 over CEC derived from four modelled results.

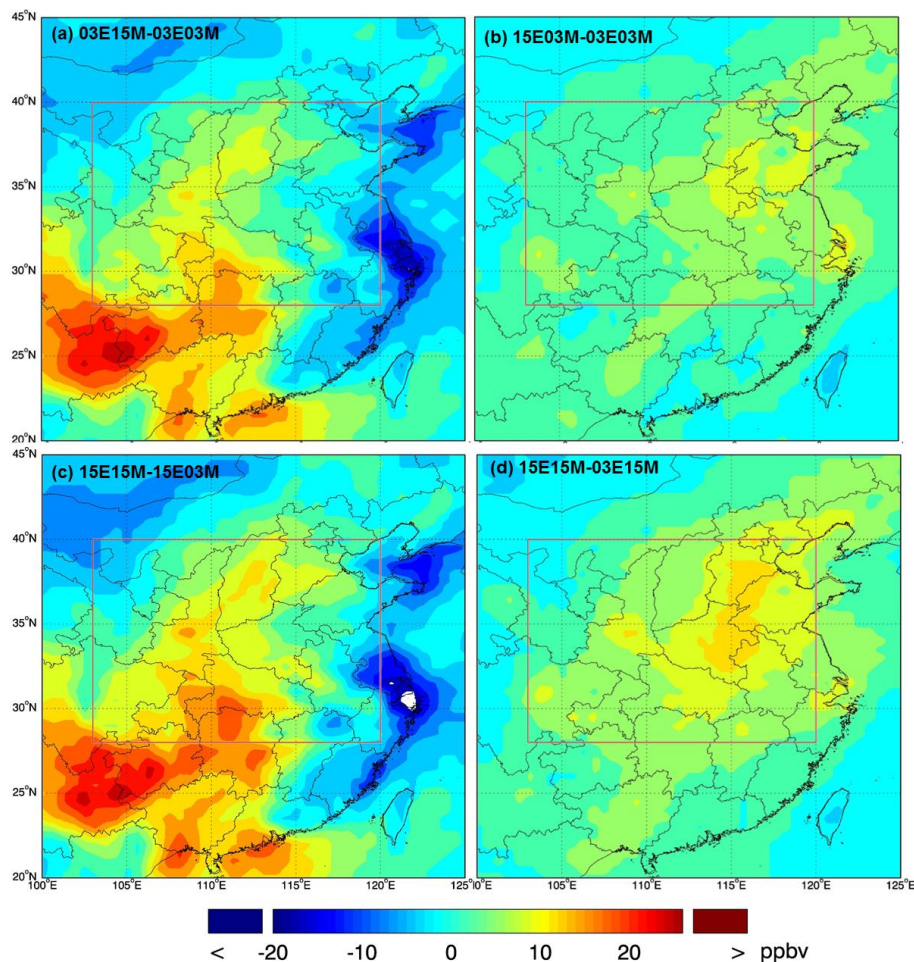


Figure 5. (a) Contributions of meteorological changes to surface MDA8 O₃, comparing 03E15M and 03E03M (2003 standard) simulations; (b) Contributions of emission changes to surface MDA8 O₃, comparing 15E03M and 03E03M (2003 standard) simulations; (c) Contributions of meteorological changes to surface MDA8 O₃, comparing 15E15M (2015 standard) and 15E03M simulations; (d) Contributions of emission changes to surface MDA8 O₃, comparing 15E15M (2015 standard) and 03E15M simulations.

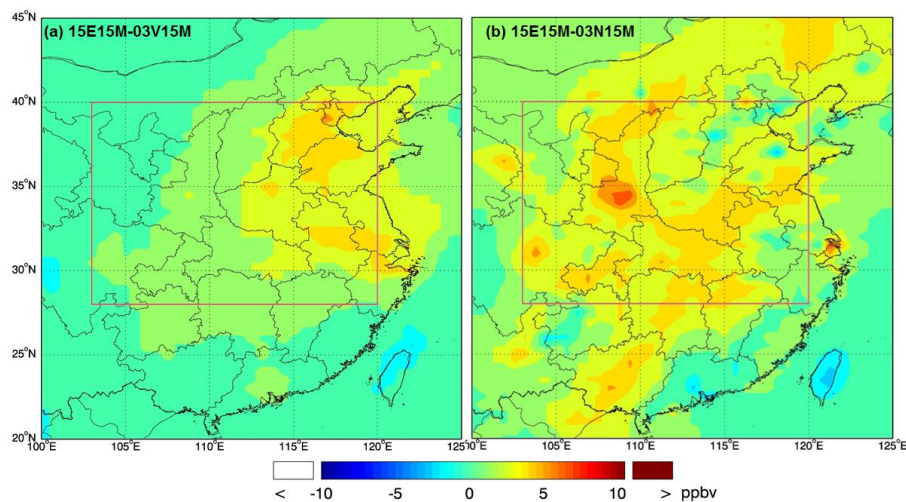


Figure 6. Effects of anthropogenic NMVOCs (a) and NO_x (b) emission changes on surface MDA8 O₃ concentrations between 2003 and 2015 when other emissions and meteorological parameters are fixed at 2015 levels.